Assessment of Post-Harvest Rice Crop Biomass and Carbon Stock using Remote Sensing Data in Google Earth Engine

Khamnoi, W.,[1] Homhuan, S.,[1*] Suwanprasit, C.[1] and Shahnawaz[2]
[1]Department of Geography, Faculty of Social Sciences, Chiang Mai University 50200, Thailand
E-mail: ms.khamnoi@gmail.com, sakda.homhuan@cmu.ac.th,* chanida.suwanprasit@cmu.ac.th
[2]Department of Geoinformatics–Z_GIS, University of Salzburg, 5020 Salzburg, Austria
E-mail: s.shahnawaz@plus.ac.at
**Corresponding Author*

DOI: https://doi.org/10.52939/ijg.v20i8.3459

Abstract
This study is motivated in response to persistent seasonal burning of rice crop-residues in various parts of Thailand. The major aims are to assess dry above ground biomass (dry-AGB) and estimate carbon stock in the rice-crop area of Buak Kang and Chae Chang subdistricts, San Kamphaeng district, Chiang Mai using Google Earth Engine (GEE), as well as develop a web platform for visualization and monitoring. The methodology includes satellite imagery and field-data acquisition, factor identification, model development, accuracy assessment, and launching an open-access web platform. The dry weight and carbon content of the sample rice plants collected during fieldwork were analyzed in a science laboratory. The study establishes a robust model for estimating dry-AGB by correlating the results from the laboratory with the backscatter coefficients of various parameters derived from Sentinel-1 imagery captured on 24.09.2023 (Ascending). The best fit model has R^2 value of 0.852, which estimated total 16019.13 Tons dry-AGB and 3524.21 Tons carbon stock in the total identified rice-crop area of 34.61 km². The GEE apps based web platform facilitates calculation and visualization of dry-AGB and carbon stock supporting effective monitoring and management of rice-crop in the study area.

Keywords: Above Ground Biomass, Carbon stock assessment, Crop residue burning, Google Earth Engine, Multiple regression analysis, SAR imagery

1. Introduction

The large scale burning of crop residue in agricultural fields is a perpetual practice in many countries, including Thailand, which causes seasonal increase of air pollution to dangerous levels. Such activities not only pause serious threats to several aspects of human health but also infuse enormous amount of greenhouse house gases into the atmosphere and add to the factors of climate change significantly [1] and [2]. Rice is a vital staple food in Thailand and a key agricultural product not only for domestic consumption but also for export purposes. Depending on the availability of sufficient water either from rains or from various irrigation facilities, it is cultivated during two different phases of time in a year known as 'main-season' and 'off-season' cropping. The main-season coincides with the rainy season and this crop takes about 120-140 days to mature from planting to harvesting stage. Usually, the planting time spreads from late May till late August and the harvest time lasts from late September till late December. The whole process of the off-season cropping takes about 90-100 days mostly from January till April. The countrywide gross rice cultivation area in 2022 was nearly 11.6 million hectares i.e. about 49% of the gross cropped area. Close to 80% of the gross rice crop area is sown during the main season and this provides approximately 82% of the country's total annual rice production weighing about 33 million tons [3] and [4]. Besides, it produces nearly 42 million tons of aboveground biomass (AGB) annually, and about 70% of this is burned in the fields after harvest [5].

The open air burning of rice-crop residue in the fields is widespread in northern Thailand, especially in Chiang Mai province, and this is the primary driver of dangerously high levels of seasonal air pollution in the region as well as in the adjacent parts of the neighboring countries [6].

This combustion not only releases smoke and harmful gases in the air but also infuses fine particles of carbon and other types of solid matter. Such air pollutants cause potential health risks of various types and degrees which include respiratory diseases, allergies, hypertension, and lung cancer etc. The worsening situation prompts various international agencies and local governments to prioritize air quality monitoring and improvement [7] and [8] and this requires precise estimation of AGB for planning and implementing appropriate measures. As mentioned previously, the rice cultivation activities occur intermittently at many places located in different parts and spread over several months so employing geospatial approach seems most appropriate for spatial-temporal analysis for affective decision making.

Currently, various types of technologies providing tools for accessing and analyzing the data required for understanding and tackling the environmental issues are available to government agencies, private organizations as well as the general public. Cloud computing is one such service offered by several vendors facilitating online data storage, retrieval, processing and analyzing capabilities. This type of infrastructure reduces the complexity of establishing and maintaining in-house facilities, lowers budgetary costs significantly, and saves time immensely. The users can utilize relevant cloud services from any location and access the open data they want to process according to their needs. The Google Earth Engine (GEE) platform facilitates access to various types of open geospatial datasets, including a wide range of satellite images of fine to coarse resolutions. It channelizes the capabilities of Google Cloud Machine Learning Engine enabling the processing and analysis of geospatial datasets for various spatial and temporal applications on the Earth's surface from global to local scales [9]. The GEE also provides access to the C-Band Synthetic Aperture Radar (SAR) images captured by Sentinel-1 satellite in all weather conditions during both day and night times. The 10 meter spatial resolution SAR images of VH and VV polarization contain backscatter signals of both surface and volume of the observed objects. This capability, combined with field based observations, enhances the accuracy in assessing AGB and can be effectively utilized for various practical applications [10][11][12] and [13]. The integrated modeling capabilities of GEE can be leveraged for developing statistical models establishing correlations between SAR backscatter coefficients (BC) values and field based observations for estimating rice crop height and AGB [14].

However, these methods have remained underutilized, and validation across more diverse field observation sites could enhance their reliability. Further research addressing these gaps would help develop more robust and transferable models for rice crop monitoring and estimation [15]. Therefore, this research aims to achieve the two main objectives i.e. (i) assessment of post-harvest rice-crop Above Ground Biomass (AGB) and estimation of its carbon stock, and (ii) launch a web platform for online calculation, visualization and monitoring of rice-crop AGB and carbon stock. By leveraging the applications of Sentinel-1 datasets and GEE based processing, this study aims to devise a low cost alternative approach to assess and monitor rice-crop AGB efficiently for effective management strategies.

2. Study Area

The study area includes two sub-districts of San Kamphaeng district, namely Buak Kang and Chae Chang, situated in Chiang Mai province of Thailand and these extend from 99°04′3″E to 99°10′54″E longitudes and 18°40′07″N to 18°44′30″N latitudes (Figure 1). The combined geographical area of the two sub-districts is around 47 km² i.e. Buak Kang around 30 km² and Chae Chang nearly 17 km². The topography is predominantly flat, intersected by two irrigation canals that derive substantial water for agricultural activities from Mae Kuang and Mae On reservoirs. Agriculture is the primary occupation of the local population and about 73% of the total area, i.e. 34.61 km², is devoted to rice cultivation. Depending on the cropping season and market prices, the farmers cultivate four varieties of rice in the study area namely San-Pah-Tawng-1, RD-MAEJO2, CPRICE888, and Riceberry.

Also, Buak Kang and Chae Chang sub-districts are included in a large-scale agricultural initiative of the Government for promoting collaborative efforts among the local farmers in production, management, and marketing of rice. This program aims to reduce production costs, enhance production efficiency, and improve competitiveness with support from relevant governmental agencies and other organizations. Considering the factors of rice cultivation management, these two subdistricts make an optimal case for the assessment of dry-AGB and carbon stock in the rice-crop area.

3. Data Acquisition and Pre-Processing

The study is based on two sources of data i.e. images obtained from 2 different satellites and the data collected through an intensive field Survey and extending over several months.

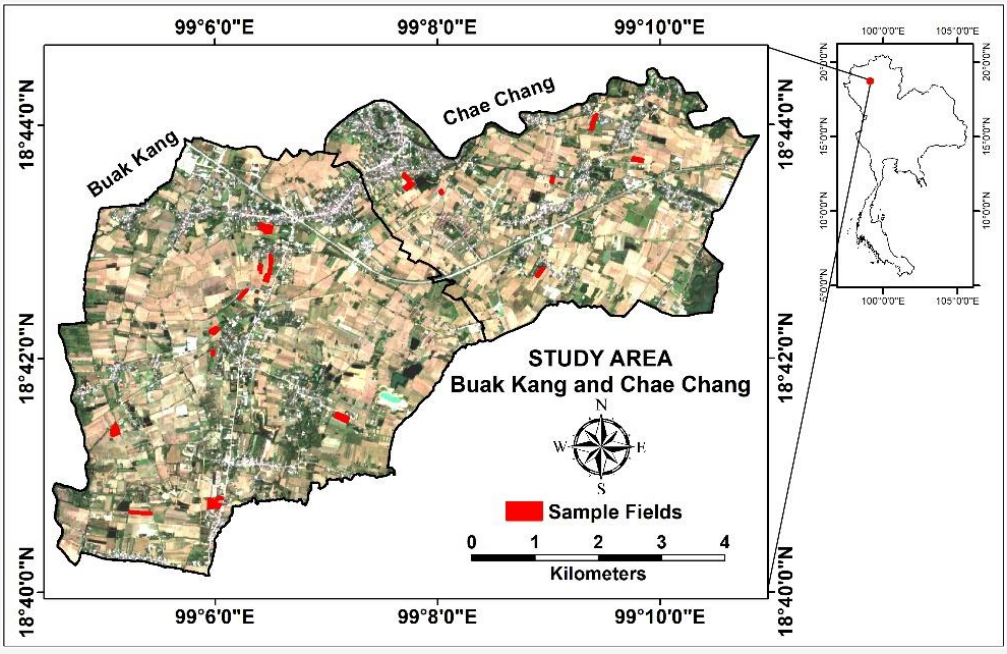

Figure 1: Buak Kang and Chae Chang sub-sistricts, San Kamphaeng district, Chiangmai

Table 1: Details of satellite imagery used in the study

Date	Satellite	Scene ID	Band
21-09- 2023	Sentinel-1	COPERNICUS/S1_GRD/S1A_IW_GRDH_1SDV_20230921T231630_20230921T231655_050432_0612B3_053E	VV and VH
24-09- 2023	Sentinel-1	COPERNICUS/S1_GRD/S1A_IW_GRDH_1SDV_20230924T113046_20230924T113111_050469_0613F7_A797	VV and VH
20-11- 2023	Sentinel-2	COPERNICUS/S2_SR_HARMONIZED/20231120T035039_20231120T040107_T47QNA	R, G, B, VNIR

Sentinel-1 dataset contains GRD scenes processed to remove the thermal noise, radiometrically calibrated, and terrain corrected using the ASTER DEM. Further details can be accessed at: https://developers.google.com/earth-engine/datasets/catalog/COPERNICUS_S1_GRD#bands.
Sentinel-2 dataset contains harmonized surface reflectance products, processed to Level-2A with atmospheric correction applied. Further details can be accessed at: https://developers.google.com/earth-engine/datasets/catalog/COPERNICUS_S2_SR_HARMONIZED.
VV = Single co-polarization, vertical transmit/ vertical receive; VH = Dual-band cross-polarization, vertical transmit/ horizontal receive; R = Red; G = Green; B = Blue; VNIR = Visible Near Infra-Red.

3.1 Satellite Image Selection and Pre-Processing

This includes the images acquired by Sentinel-1 and Sentinel-2 satellites (Table 1). Sentinel-1 is equipped with a SAR instrument operating at a frequency of 5.405 GHz providing spatial resolution of 10-meter [16]. This dataset includes Ground Range Detected (GRD) images and incorporates Sentinel-2 imagery to aid the land use-land cover classification process [17]. The 'Sentinel-1 Toolbox' within the GEE platform was used to process the GRD images for thermal noise removal, radiometric calibration, and terrain correction. The Advanced Spaceborne Thermal Emission and Reflection Radiometer Digital Elevation Model (ASTER DEM) data was used for terrain correction. Finally, the terrain-corrected values were converted to decibels through logarithmic scaling $10\log_{10}X$ [18]. Within GEE, the Sentinel-1 imageries captured during the harvest stage of rice-crop were filtered according to the boundaries of the study area. The filtering utilized ascending and descending orbits of Santinel-1 for pre-harvest and post-harvest periods in September 2023. The spatial filtering techniques such as boxcar or median filters were applied to reduce speckle noise in Sentinel-1 and Sentinel-2 imageries.

Additionally, analysis of the difference between VV and VH polarizations of the two Sentinel-1 images was conducted to generate images with consistent 'smooth (sm)' values across each image. The Sentinel-2 bands were combined with Sentinel-1 GRD images for enhancing the accuracy of non-rice and rice-crop area classification.

3.2 Field Data Collection and Pre-Processing

The research team conducted several rounds of intensive field surveys in the study area from September to November 2023 for collecting sample rice plants and other relevant details, in order to assess the biomass and carbon stock. Following a multi-stage stratified sampling scheme, 30 ready-to-harvest rice fields were selected in the two sub-districts (Figure 1). The number of selected fields were proportionate to the area under rice cultivation in each sub-district i.e. 20 fields in the Buak Kang with 22.54 km² of rice-crop area and 10 fields in Chae Chang having about 12.1 km². Also, the prevalence of rice varieties cultivated in each sub-district was taken into consideration while selecting the rice crop fields. Thereafter, 5 sample plots of 1 by 1 meter, i.e. 1 m², were marked in various parts of each selected field for collecting relevant details from the total of 150 sample plots (Figures 2(a) and 2(b)). The parameters recorded included total number of rice plants in each sample plot, height of the whole above ground part of the plant and height of the stubble after harvesting. Further, certain number of whole rice plants were collected from each sample plot based on their height i.e. four plants per plot for the plants taller than 130 cms, five plants for height between 120 cms and 130 cms and six plants for shorter than 120 cms. The data of all the five sample plots in each of the 30 selected fields were averaged to represent the overall parameters of the corresponding sample fields. Also, the relevant spatial information was recorded for the 150 sample plots as well as for another set of 200 spots for capturing the various stages of rice plant growth above ground to be used as the 'Region of Interest (ROI)' in the object bases image classification process.

The sample rice plants, as and when collected during the field work, were sent to the science laboratory at the Faculty of Agriculture, Chiang Mai University, Thailand for analyzing their dry-AGB weight and Carbon Content. For dry-AGB weight, the sample plants were placed in a hot air oven at 105 degrees Celsius for 48 hours [19]. For determining Carbon Content, the dry-AGB of each of the 30 sample fields was finely ground and analyzed separately using combustion method in multi EA 4000 instrument [20].

4. Methods of Data Processing and Analysis

This study combines remote sensing data with fieldwork observations for identifying the total rice-crop area as well as for comprehensive assessment of dry-AGB and carbon stock in the rice fields. The complete workflow of methodology from acquiring the required data till obtaining the final results involved several steps (Figure 3). The image processing and analysis steps were carried out on cloud-based computing system through GEE platform.

4.1 Classification of Non-Rice Area and Rice-Crop Area

Identification of rice-crop area is the basic requirement for assessing total above rice-crop AGB and carbon stock in the study area. It has been found that the reflectance coefficient of rice-crop in the optical satellite images generally increases as the crop matures over time which suggest a positive correlation between the two [21]. Also, the SAR imageries are highly reliable for identifying rice-crop area and capturing various stages of crop growth (Figure 2(a)) by analyzing the BC values of VV and VH bands, in relation to various crop parameters [22]. In this study, both SAR and optical images have been used (Table 1). The selected optical image of Sentinel-2 had less than 5% cloud cover which were masked with the help of QA60 band for avoiding the potential errors. The image classification was performed through Object Based Image Analysis (OBIA) approach [23]. This process requires segmentation of the selected images and identification of the segments representing various Land Use Land Cover (LULC) classes to be used as 'Region of Interest (ROI)' for classification and validation process. The images were segmented with the help of simple non-iterative clustering (SNIC) algorithm by defining five parameters which are (i) compactness = 0.1, (ii) connectivity = 8, (iii) neighborhood size = 10, (iv) size = 5, and (v) seeds = null. Each parameter serves a specific purpose i.e. 'Compactness' affects the shape of the clusters, with higher values resulting in more compact, square-shaped clusters; 'Connectivity' defines the type of connection among adjacent objects; 'Neighborhood Size' helps avoiding tile boundary artifacts and determines the size of adjacent objects; and 'Size' determines the spacing of the superpixel seed locations. The 'Random Forest Classifier' algorithm was used for grouping the image segments into 2 broad LULC classes i.e. (i) non-rice area, and (ii) rice-crop area.

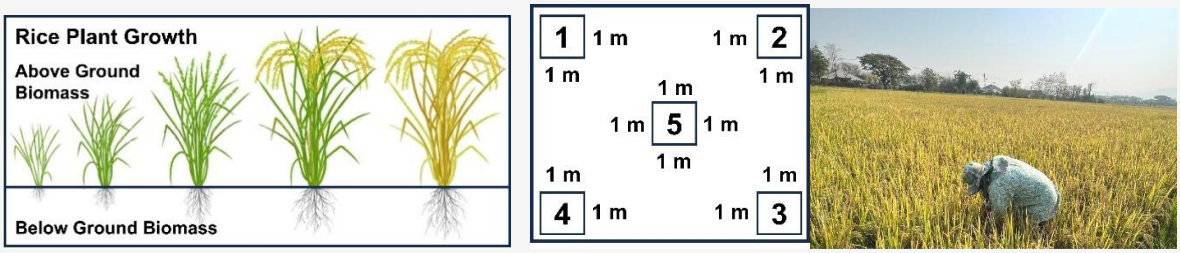

(a) (b)

Figure 2: (a) growth stage of rice plant (b) rice sampling in the rice field

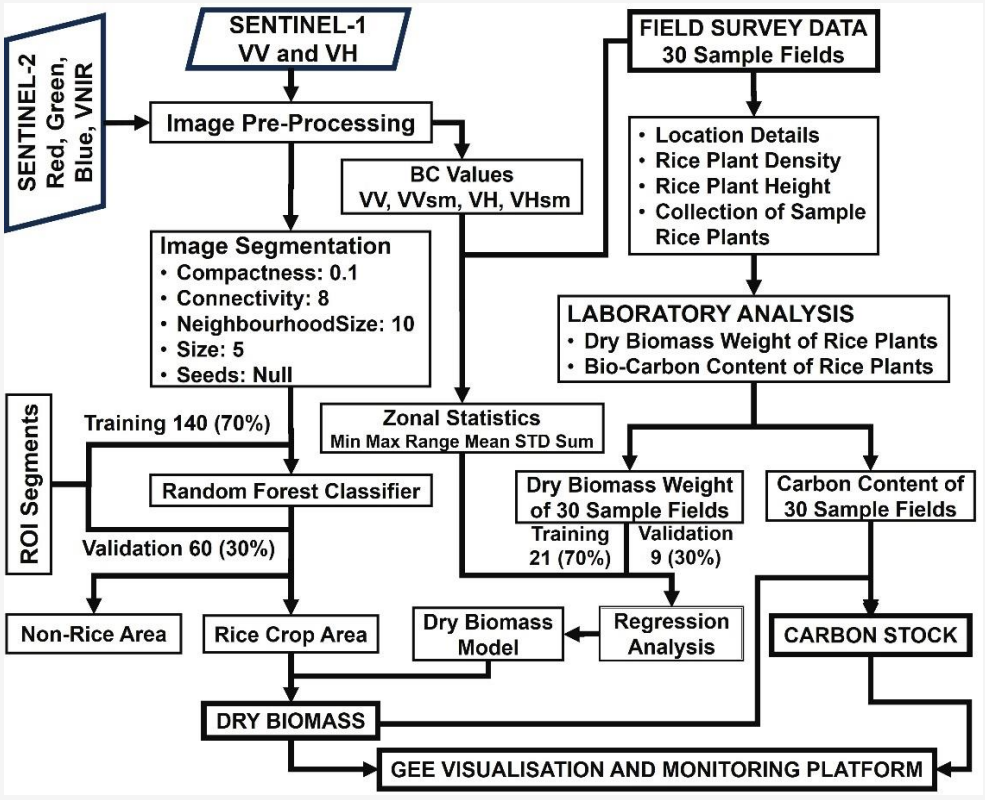

Figure 3: Flow-diagram of methodology

Total 200 segments representing 2 broad LULC classes were identified as ROI, out of which 140 (70%) were used as training samples for classification and 60 (30%) for validation. Also, confusion matrix and error matrix were calculated for assessing the accuracy of the classification. Finally, 'rice-crop area' was extracted and 'morphological reducer filter' was applied to clean-up the size and boundaries of the obtained segments.

4.2 Zonal Statistics Analysis

This is a type of spatial analytical technique for performing several statistical calculations on the attributes of a spatial dataset according to the predefined boundaries of smaller areas or zones within a larger study area. This approach facilitates comparison of spatial variations in the selected parameters within a study area minimizing the potential errors in generalization emanating from the variations due to other influencing factors [24]. As stated, the study aims at assessing dry-AGB and carbon stock in the rice-crop area using Sentinel-1 images. This requires analysis of relationship between dry-AGB and carbon stock on one side and various BC values obtained from Sentinel-1 images on the other side. Since carbon stock is a certain proportion of the dry-AGB so the dry-AGB weight of the sample rice plants analyzed in the laboratory serves as dependent variable and 'Zonal Statistics' of various BC values of Sentinel-1 images extracted according to the boundaries of the 30 sample rice fields serve as independent variables.

Total 48 independent variables were used for developing the regression model and Table 2 shows the 6 types of 'Zonal Statistics' calculated from the raw and smoothed (sm) BC values of 2 bands (VV & VH) of the selected Sentinel-1 images for two different dates.

Multiple regression analysis is a widely used statistical method for modelling the relationship between a dependent variable and more than one independent variables [25]. The study used 'Stepwise Multiple Regression Method' (Equation 1) taking 21 (70%) of the sampled 30 dry-AGB estimates for training the model and 9 (30%) for validation.

$$Y = a + b_1x_1 + b_2x_2 + b_3x_3 + \ldots + b_nx_n$$

Equation 1

Where: Y is dry-AGB, while $x_1, x_2, x_3, \ldots, x_n$ represent the n independent variables from Table 2. Multiple regression analysis calculates the weights, $a, b_1, b_2, b_3, \ldots, b_n$ to optimize the prediction of the dependent variable based on the independent variables. This optimization is typically achieved through least squares estimation.

The correlation coefficient quantifies the strength and direction of a linear association between two variables, with coefficient values ranging from -1 (perfect negative correlation) to +1 (a perfect positive correlation) and a coefficient of 'Zero' implies that there is no correlation between the variables. The categories of positive correlation are defined as follows: very strong positive (0.80 to 1.00), strong positive (0.60 to 0.79), moderate positive (0.40 to 0.59), weak positive (0.20 to 0.39), and very weak positive (0.00 to 0.19) [26]. The same is represented for negative correlation with the 'minus' sign. The calculation of carbon stock was adapted using Module C-CS, which provides its estimation across various carbon pools. This module includes guidelines for calculating plot areas, applying statistical methods, and analyzing the data, all of which are essential for precise assessments of dry-AGB and carbon stock [27]. Carbon stock per unit area is defined in equation 2.

$$Cs = C \times DryAGB$$

Equation 2

Where: Cs represents the carbon stock per unit area (kgC/m²), $DryAGB$ denotes the weight of dry-AGB per unit area (kg/m²) derived from multiple linear regression, and C is the percentage of carbon content obtained through laboratory analysis of sampled rice plants.

4. Results and Discussion

4.1 Image Classification

The research team tested various SNIC parameters for obtaining high accuracy of non-rice area and rice-crop area classification. The best performing SNIC parameters were optimized for segmentation of the combined images from Sentinel-1 and Sentinel-2. The optimal parameters were identified to be: compactness (0.1), connectivity (8), neighborhood size (10), and size (5). The Random Forest Classifier identified the results show rice-crop area of 34.61 km² in the total area of about 47 km². It achieved an overall accuracy of 96%, indicating that it correctly classified the majority of the superpixels. The Kappa value of 0.93 suggests a very high level of agreement between the observed and predicted 2 broad LULC classes, significantly exceeding what would be expected by chance. These metrics underscore the effectiveness of combining SNIC for image segmentation with Random Forest Classifier for identifying rice-crop area.

Table 2: Variables used in the regression equation

1 Dependent Variable	48 Independent Variables
Dry Above Ground Biomass Weight (dry-AGB)	2 Image Capture Dates: 0921 (September 21, 2023), and 0924 (September 24, 2023) Total 48 independent variables: 2 * 4 * 6 = 48 - 2 Image Capture Dates: 0921, 0924 - 4 types of BC values: VV, VVsm, VH, VHsm - 6 types of Zonal Statistics values: Min, Max, Mean, Range, STD, Sum Example-1: VV0921Min; VVsm0921Min; VH0921Min; VHsm0921Min etc. Example-2: VV0924STD; VVsm0924STD; VH0924STD; VHsm0924STD etc.

4.2 Modelling of Dry-AGB based on Backscatter Coefficients (BC) of Sentinel-1 Images

As mentioned previously, the dry-AGB of the sample rice-crop plants collected from the 5 plots of one square meter in each of the 30 sample fields was analyzed in a science laboratory. Depending on the average height and species of the sample rice-crop plants, the average dry-AGB weight varied between 141.7 to 522.75 g/m² giving an average of 330.6 g/m². The 'Zonal Statistics' of various BC values falling within the 30 sample rice fields demonstrate varying degrees of correlation with dry-AGB. Figure 4(a) illustrates that *VV0921Max* has a weak positive correlation (0.31) with dry-AGB, indicating that higher maximum values of VV are not much associated with the higher dry-AGB. Conversely, *VH0921Max* shows a weak negative correlation (-0.39) with dry-AGB, suggesting that higher maximum values of VH correspond to lower dry-AGB. Figure 4(b) reveals that *VV0924Max* and *VV0924Mean* have strong positive correlation with dry-AGB having the 'r value' of 0.72 and 0.63 respectively. However, *VH0924Max* shows a negative correlation of (-0.46) the correlation coefficient (r) between dry-AGB and BC values derived from the ascending pass on 24.09.2023 (r = 0.923) is the highest (Table 3). The multiple regression models for estimating dry-AGB in the rice fields using Sentinel-1 images of 2 different dates are presented in Table 3. The model for '21.09.2023 (Descending)' image explains only 22.9% variance in dry-AGB, which shows a weak significance, so this has been discarded from further analysis. On the other side, the model for 24.09.2023 (Ascending) image, incorporating four independent variables (i.e. $VHMax$, $VHMin$, $VHsmMax$ and $VVsmMax$), gave a highly reliable R^2 of 0.852.

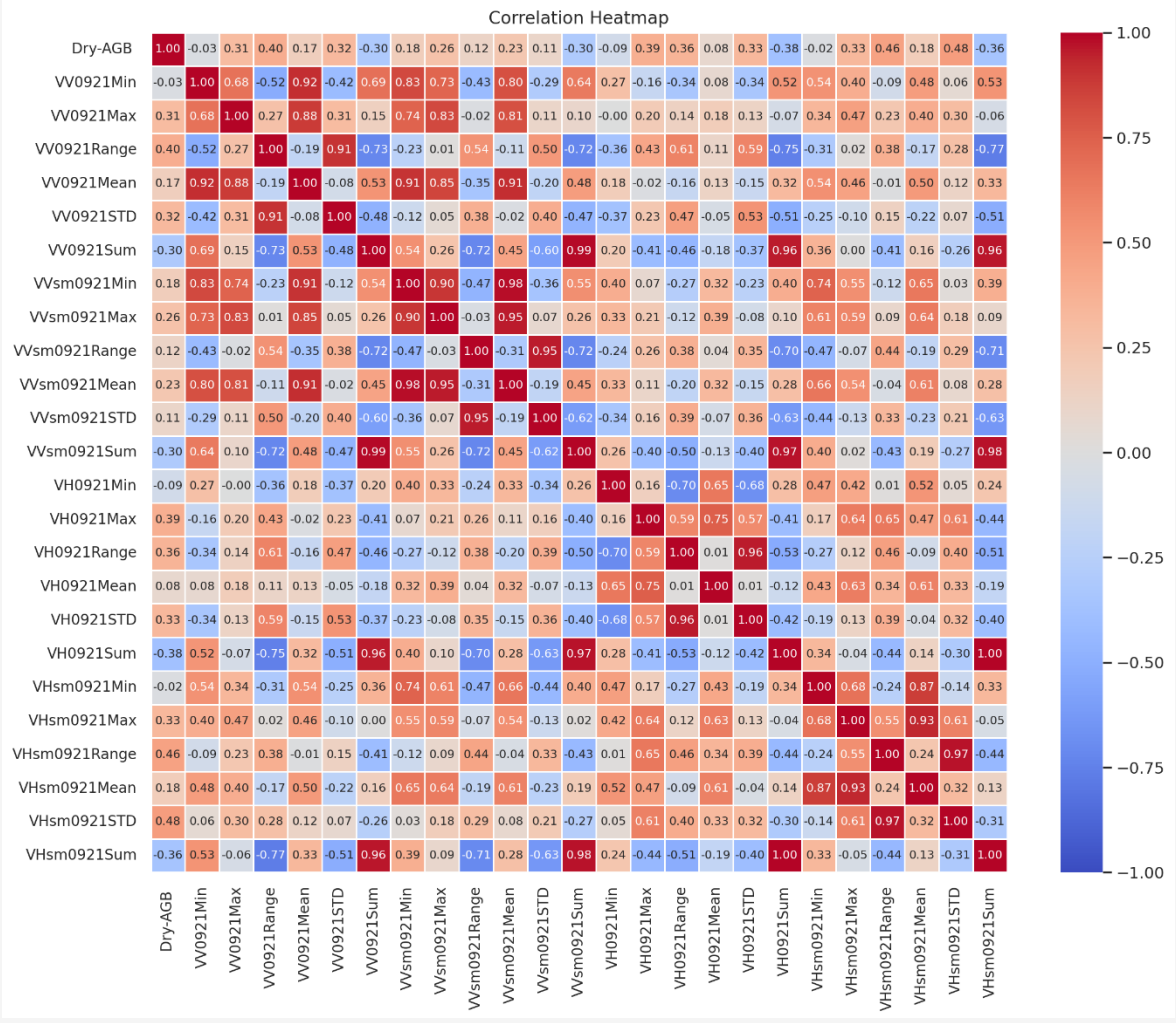

Figure 4: Cross-correlation coefficients between dry-AGB and Sentinel-1 BC parameters: (a) Descending pass on 21.09.2023 (Continue next page)

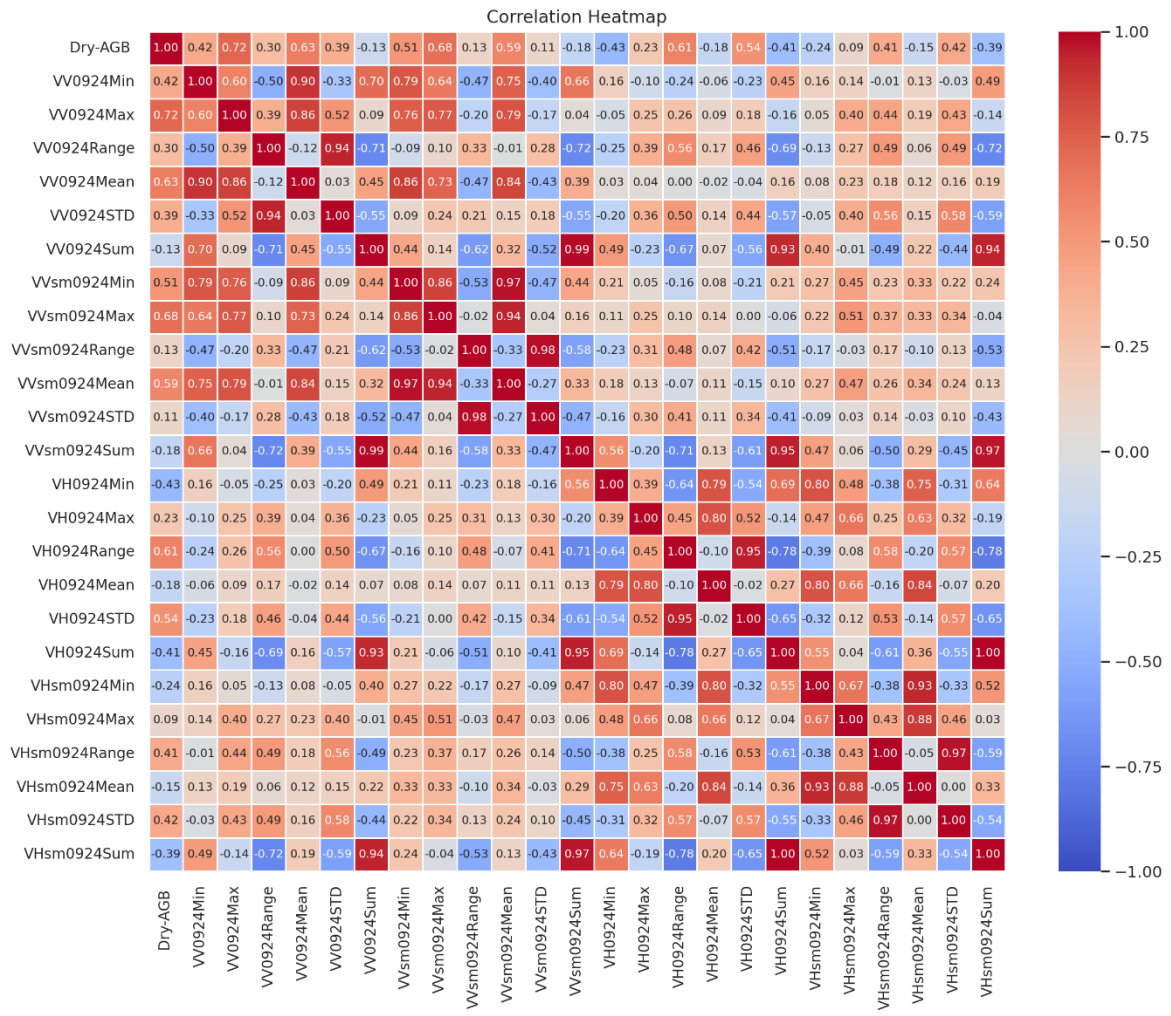

Figure 4: Cross-correlation coefficients between dry-AGB and Sentinel-1 BC parameters: (b) Ascending pass 24.09.2023 (Continue from previous page)

Table 3: The regression equations derived for predicting dry-AGB

Sentinel-1 Image	Regression model	R	R^2	Adjusted R^2	F-value	Sig.
21.09.2023 (Descending)	$18.722VHsmSTD + 27.329$	0.479	0.229	0.189	5.659	0.028
24.09.2023 (Ascending)	$26.586 + 2.196VHMax + 2.032VHMin - 3.139VhsmMax + 5.166VvsmMax$	0.923	0.852	0.816	23.105	0.000

Leaving aside $VVsmMax$, the other three variables show a positive relationship of varying degrees with dry-AGB whereas $VVsmMax$ shows a negative coefficient of -3.139. A positive relationship denotes that a rise in the BC value of an independent variable leads to a rise in the amount of dry-AGB by the modelled coefficient factor of that particular variable. For example, $VHMax$ (maximum vertical height) has coefficient value of 2.196 and this means that one-unit rise in the BC value of $VHMax$ shows a rise of 2.196 units in dry-AGB. The same applies to $VHMin$ and $VVsmMax$ having corresponding positive coefficients of 2.032 and 5.166. The case of a negative relationship is opposite that a rise in the BC value of an independent variable leads to a decrease in the amount of dry-AGB by the modelled coefficient factor of that particular variable. The intercept of this regression models is 26.586 and this shows the expected value of dry-AGB when BC values of all independent variables are 'Zero'.

This may happen if the crop is still in the early stage of growth or the crop has been harvested and only small stubble and some thrashed straw is remaining in the fields. These observations highlight the importance of using multi-temporal and multi-polarization satellite data to reliably estimate dry-AGB and corresponding carbon stock in the rice-crop area.

The application of linear regression algorithms in machine learning, specifically multiple linear regression, has demonstrated considerable efficacy in predicting the AGB of rice-crop [28][29][30][31] and [32]. This study has identified significant positive relationships between dry-AGB of rice-crop and BC of selected parameters notably, *VHMax*, *VHMin*, *VHsmMax*, and *VVSMax*, and this demonstrates strong potential of SAR and other Remote Sensing data for assessing AGB. This aligns with the findings of various previous studies that show a positive correlation between AGB and the derived coefficients [33][34] and [35]. Also, some studies compared and developed different algorithms to find low computational costs and achieving high accuracy in predicting AGB using C-Band SAR channels. Besides, it is observed that a low correlation may result from BC values influenced by surface roughness, signal noise, and vegetation structure causing complex interactions between radar signals and surface characteristics [36] and [37].

4.3 Assessment of Dry-AGB and Carbon Stock in the Rice-Crop Area

The model developed for Sentinel-1 image of 24.09.2023 (Ascending), demonstrated the highest correlation coefficient ($R^2 = 0.852$), thus, it was fitted in multiple linear regression equation for calculating dry-AGB of rice-crop. The distribution of assessed dry-AGB and carbon stock in various categories of rice-crop area are presented in Table 4 and Figures 5(a) and 5(b). The total dry-AGB assessed for the entire rice-crop area, i.e. 34.61 km², is 16019.13 Tons and there are significant variations in its spatial pattern (Figure 5(a)).

Table 4: Dry-AGB and carbon stock assessed from Sentinel-1 image of 24.09.2023 (Ascending)

Dry-AGB (kg/100 m²)	Area (km²)	Area (Percent)	Dry-AGB (Total Tons)	Carbon Stock (kgC/100 m²)	Area (km²)	Area (Percent)	Carbon Stock (Total Tons)
> 90	0.03	0.08	28.82	> 25	0.00	0.00	0.05
75 - 90	0.06	0.19	54.67	20 - 25	0.03	0.08	6.29
60 - 75	1.40	4.03	953.95	15 - 20	0.26	0.76	45.52
45 - 60	12.94	37.40	6978.78	10 - 15	13.50	39.01	1644.17
30 - 45	17.93	51.81	7391.96	5 - 10	20.39	58.90	1809.12
< 30	2.25	6.49	610.94	< 5	0.43	1.25	19.06
Total	**34.61**	**100.00**	**16019.13**	**Total**	**34.61**	**100.00**	**3524.21**

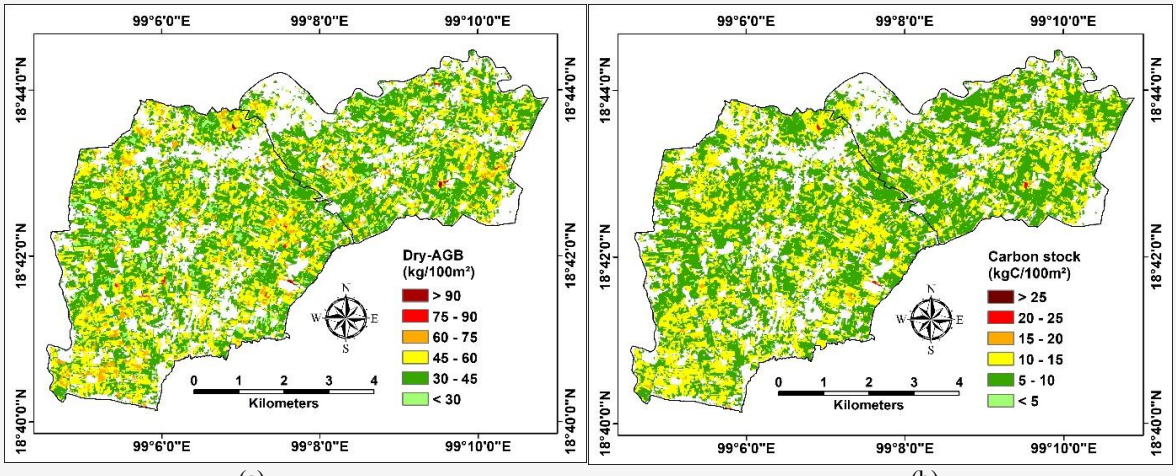

(a) (b)

Figure 5: (a) dry-AGB (b) carbon stock

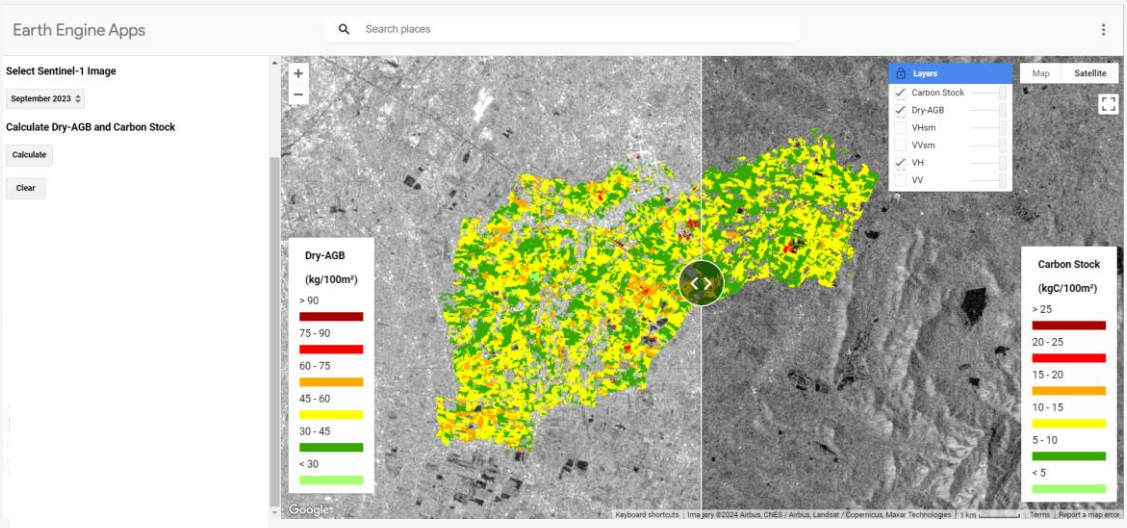

(a)

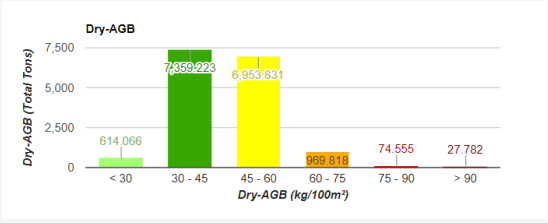

(b)

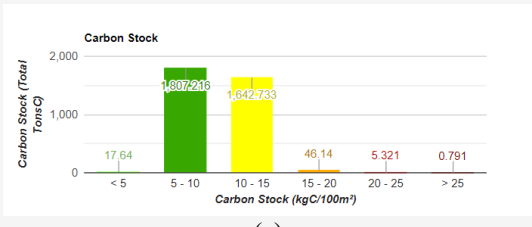

(c)

Figure 6: GEE app-based platform for visualization and monitoring of dry-AGB and carbon stock (a) The overview of dry-AGB and carbon stock platform (b) dry-AGB chart in platform (c) carbon stock chart in platform (https://wpwn-gps.projects.earthengine.app/view/dry-agb-and-carbon-stock-monitoring-system)

The quantity of dry-AGB in 17.93 km² (51.81%) rice-crop area varies between 30 to 45 kg/100m² and total dry-AGB in this part is 7391.96 Tons. Second to this, 12.94 km² (37.40%) area has variation of dry-AGB between 45 to 60 kg/100m² and its total weight is 6978.78 Tons. The total amount of dry-AGB in the remaining 4 km² (11%) rice-crop area is 1648.38 Tons. The spatial variations in the dry-AGB are caused mainly by the differences in the growth-stage plants in the rice-crop area which is affected by the timing of plantation stretching from May to August. The carbon stock in the total rice-crop area is estimated to be 3524.21 Tons. The prevalence of carbon stock corresponds to dry-AGB so the spatial patterns of the both are quite similar (Figure 5(b)). The carbon stock corresponding to the dry-AGB of the 30 sample fields analyzed in the laboratory ranged from 31.53 to 116.31 g/m² whereas the average value was 72.56 g/m². The carbon stock in 34.32 km² (99.16%) of total rice-crop area varies between 5 and 15 kgC/100 m², and the total stock in this area is about 3472.40 (98.53%) Tons out of the total carbon stock in the entire rice-crop area. Although the values modelled for assessing dry-AGB and carbon stock are quite consistent with similar previous studies [38], however, some variations can be explained due to various varieties of rice [39] and resultant straw after threshing [40].

5. GEE Platform for Visualization and Monitoring

A web platform for visualization and monitoring of dry-AGB and carbon stock using GEE apps has been developed (Figure 6). It facilitates cloud-computing based semi-automatic processing and analysis of the selected satellite images combined with the relevant data modelling steps, significantly reducing the time and effort required for manual data handling, thus, enhances cost-effectiveness. The platform is enabled for calculations and displays of dry-AGB and carbon stock derived from Sentinel-1 images of September month in each year, beginning from 2023 onwards. Although, it is possible to display different layers integrated in the platform as a background but analysis of dry-AGB and carbon stock is based only on the parameters of Sentinel-1 image used in the model i.e. *VHMax*, *VHMin*, *VHsmMax*, and *VVSMax* (Figure 6(a)). Apart from displaying the spatial distribution maps of the two aspects, the platform also contains bar graphs showing the total amount of

dry-AGB (Figure 6(b)) and carbon stock (Figure 6(c)) within various categories. This user-friendly platform not only supports the monitoring and decision-making processes of various government, non-government and marketing agencies but also helps informing the state of their rice crop to the local farmers as well as sensitizing them about their role in generating the harmful effects of on-field burning of crop residues.

It has been demonstrated that integrating satellite imagery and statistical analysis techniques for predictive modeling can effectively assess and monitor agricultural crop production, which is crucial for agricultural management and production planning [41]. The development of online applications facilitates resource managers and stakeholders' access to and use of up-to-date information, indicating that combining satellite data with cloud-based processing platforms like GEE can significantly enhance resource monitoring and management [42][43] and [44]. However, there is a need to update the model periodically for keeping the accuracy of assessment at higher levels.

6. Summary

Rice is a widely cultivated crop in Thailand and many other parts of the world. Along with edible grains, the crop also produces huge amounts of post-harvest crop-residues, and the farmers usually burn a very large part of it in the fields themselves. The open-air crop-residue burning has a range of direct and indirect harmful effects on human health, atmosphere, environment and climate change. Thus, a system for assessing and monitoring the spatial and temporal patterns of rice-crop AGB and its carbon stock is needed for affective management. This study provides methodology for assessing dry-AGB and carbon stock in rice-crop area using SAR images. A multiple regression model was developed by integrating 48 BC parameters derived from 2 Sentinel-1 images but the most accurate predictor of dry-AGB was associated with the image of 24.09.2023 (Ascending). Its R^2 value was 0.852 and it incorporated only 4 BC parameters (i.e. *VHMax*, *VHMin*, *VHsmMax*, and *VVSMax*), 3 of which has a positive relationship and one, $VHsmMax$, has negative relationship.

The total dry-AGB in the whole rice-crop area of 34.61 km^2 was assessed to be 16019.13 Tons showing significant spatial variations, the dry-AGB on 89% of the total rice-crop area varies between 30 and 60 kg/100 m^2. Corresponding to this, the carbon stock in the total rice-crop area is estimated to be 3524.21 Tons and this varies between 5 and 15 kgC/100 m^2 on 99.16% of total rice-crop area. A cloud-computing based user-friendly GEE app platform has been developed for calculating pre-modelled dry-AGB and carbon stock of rice-crop from Sentinel-1 imagery of the study area. In conclusion, this study makes significant methodological and technological contributions to the field of agricultural monitoring and provides a scalable, efficient open-access platform assessing AGB and carbon stock for informed policy formulation and affective management planning.

Acknowledgments

This work was supported by the ERASMUS+ KA107: Student and Staff Mobility program. We extend our gratitude to the European Commission and the University of Salzburg for facilitating this mobility, and to the Chiang Mai University for continued support throughout this project.

References

[1] Singh, Y., Sharma, S., Kumar, U., Sihag, P., Balyan, P., Singh, K. P. and Dhankher, O. P., (2024). Strategies for Economic Utilization of Rice Straw Residues into Value-Added By-Products and Prevention of Environmental Pollution. *Science of the Total Environment*, Vol. 906(167714). https://doi.org/10.1016/j.scitotenv.2023.167714.

[2] Tipayarom, D. and Oanh, N. T. K., (2007). Effects from Open Rice Straw Burning Emission on Air Quality in the Bangkok Metropolitan Region. *Science Asia*, Vol. 33(3), 339-345. https://doi.org/10.2306/scienceasia1513-1874.2007.33.339.

[3] National Statistical Office, (2023). Statistical Year Book - Thailand. Ministry of Digital Economy and Society, Thailand. [Online]. Available: https://www.nso.go.th/public/e-book/Statistical-Yearbook/SYB-2023/6/ [Accessed June. 21, 2024].

[4] United States Department of Agriculture, (2021). Thailand Rice: Recent Dry Conditions After a Promising Start; Optimism Still Remains for this Crop Season. Foreign Agricultural Service, U.S. Department of Agriculture. Available: https://ipad.fas.usda.gov/highlights/2021/10/Thailand/index.pdf [Accessed May. 21, 2024].

[5] Hastings, T., Smyth, B., Mehta, N. and Pisutpaisal, N., (2023). Alleviating the Environmental and Economic Challenges of Rice Farming in Thailand. *Global Challenges Research Fund & Newton Fund*. Available: https://pure.qub.ac.uk/en/clippings/alleviating-the-environmental-and-economic-challenges-of-rice-far [Accessed May. 21, 2024].

[6] Kanabkaew, T. and Oanh, N. T. K., (2011). Development of Spatial and Temporal Emission Inventory for Crop Residue Field Burning. *Environmental Modeling and Assessment*, Vol. 16(5), 453–464. https://doi.org/10.1007/s10666-010-9244-0.

[7] Kumar, I., Bandaru, V., Yampracha, S., Sun, L. and Fungtammasan, B., (2020). Limiting Rice and Sugarcane Residue Burning in Thailand: Current Status, Challenges and Strategies. *Journal of Environmental Management*, Vol. 276. https://doi.org/10.1016/j.jenvman.2020.111228.

[8] Arunrat, N., Pumijumnong, N. and Sereenonchai, S., (2018). Air-pollutant Emissions from Agricultural Burning in Mae Chaem Basin, Chiang Mai Province, Thailand. *Atmosphere (Basel)*, Vol. 9(4). https://doi.org/10.3390/atmos9040145.

[9] Aji, A., Husna, V., and Purnama, S. (2024). Multi-Temporal Data for Land Use Change Analysis Using a Machine Learning Approach (Google Earth Engine). *International Journal of Geoinformatics*, 20(4), Vol. 19–28. https://doi.org/10.52939/ijg.v20i4.3145.

[10] Lasko, K., Vadrevu, K. P., Tran, V. T., Ellicott, E., Nguyen, T. T. N., Bui, H. Q. and Justice, C., (2017). Satellites May Underestimate Rice Residue and Associated Burning Emissions in Vietnam. *Environmental Research Letters*, Vol. 12(8). https://doi.org/10.1088/1748-9326/aa751d.

[11] Chang, L., Chen, Y. T., Wang, J. H. and Chang, Y. L., (2021). Rice-field Mapping with Sentinel-1a Sar Time-Series Data. *Remote Sensing (Basel)*, Vol. 13(1), 1–25. https://doi.org/10.3390/rs13010103.

[12] Shang, J., Liu, J., Chen, Z., Mcnairn, H. and Davidson, A., (2022). Recent Advancement of Synthetic Aperture Radar (SAR) Systems and their Applications to Crop Growth Monitoring. *IntechOpen*. https://doi.org/10.5772/intechopen.102917.

[13] Ndikumana, E., Ho Tong Minh, D., Dang Nguyen, H. T., Baghdadi, N., Courault, D., Hossard, L. and El Moussawi, I., (2018). Estimation of Rice Height and Biomass Using Multitemporal SAR Sentinel-1 for Camargue, Southern France. *Remote Sensing (Basel)*, Vol. 10(9). https://doi.org/10.3390/rs10091394.

[14] Sharifi, A. and Hosseingholizadeh, M., (2020). Application of Sentinel-1 Data to Estimate Height and Biomass of Rice Crop in Astaneh-ye Ashrafiyeh, Iran. *Journal of the Indian Society of Remote Sensing*, Vol. 48(1), 11–19. https://doi.org/10.1007/s12524-019-01057-8.

[15] Abdelkader, M., Bravo Mendez, J. H., Temimi, M., Brown, D. R. N., Spellman, K. V., Arp, C. D., Bondurant, A. and Kohl, H. A., (2024). A Google Earth Engine Platform to Integrate Multi-Satellite and Citizen Science Data for the Monitoring of River Ice Dynamics. *Remote Sensing (Basel)*, Vol. 16(8). https://doi.org/10.3390/rs16081368.

[16] Khamphilung, P., Konyai, S., Slack, D., Chaibandit, K., and Prasertsri, N. (2023). Flood Event Detection and Assessment using Sentinel-1 SAR-C Time Series and Machine Learning Classifiers Impacted on Agricultural Area, Northeastern, Thailand. *International Journal of Geoinformatics*, 19(6), Vol. 17–29. https://doi.org/10.52939/ijg.v19i6.2691.

[17] Google Earth Engine, (2023). Sentinel-2 MSI: MultiSpectral Instrument, Level-2A, Harmonized. [Online]. Available: https://developers.google.com/earth-engine/datasets/catalog/COPERNICUS_S2_SR_HARMONIZED [Accessed May. 31, 2024].

[18] Google Earth Engine, (2024). Sentinel-1 Algorithms.[Online]. Available: https://developers.google.com/earth-engine/guides/sentinel1 [Accessed May. 21, 2024].

[19] Saad, M. J., Sajab, M. S., Wan Busu, W. N., Misran, S., Zakaria, S., Chin, S. X. and Chia, C. H. (2020). Comparative Adsorption Mechanism of Rice Straw Activated Carbon Activated with NaOH and KOH. *Sains Malaysiana*, Vol. 49(11), 2721–2734. http://dx.doi.org/10.17576/jsm-2020-4911-11.

[20] Pham, C. T., Ly, B., Nghiem, T., Pham, T. H., Minh, N. T., Tang, N., Hayakawa, K. and Toriba, A., (2021). Emission Factors of Selected Air Pollutants from Rice Straw Burning in Hanoi, Vietnam. *Air Qual Atmos Health*. Vol. 14, 1757–1771 (2021). https://doi.org/10.1007/s11869-021-01050-6.

[21] Nontasiri, J., Dash, J. and Roberts, G., (2018). Estimating of Rice Crop Yield in Thailand using Satellite Data. *SPIE 10783, Remote Sensing for Agriculture, Ecosystems, and Hydrology XX, 107832K, September 10-13, 2018, Berlin, Germany*. http://dx.doi.org/10.1117/12.2513281.

[22] Dineshkumar, C., Kumar, J. S. and Nitheshnirmal, S., (2019). Rice Monitoring Using Sentinel-1 Data in the Google Earth Engine Platform. *MDPI AG*, Vol. 4. https://doi.org/10.3390/IECG2019-06206.

[23] Suwanprasit, C. and Shahnawaz, (2024). Mapping Burned Areas in Thailand using Sentinel-2 imagery and OBIA Techniques. *Science Report*, Vol. 14(1), 9609 (2024). https://doi.org/10.1038/s41598-024-60512-w.

[24] Cardille, J. A., Crowley, M. A., Saah, D. and Clinton, N. E., (2024). *Cloud-Based Remote Sensing with Google Earth Engine*. (2024). Springer International Publishing. https://doi.org/10.1007/978-3-031-26588-4.

[25] Wagner, M. M., Moore, A. W. and Aryel, R. M., (2006). *Handbook of Biosurveillance*. Academic Press.

[26] Meghanathan, N., (2016). Assortativity Analysis of Real-World Network Graphs Based on Centrality Metrics. *Computer and Information Science*, Vol. 9(3). http://dx.doi.org/10.5539/cis.v9n3p7.

[27] Goslee, K., Walker, S. M., Grais, A., Murray, L., Casarim, F. and Brown, S., (No Date). *Leaf technical Guidance Series for the Development of a Forest Carbon Monitoring System for REDD+ Module C-CS: Calculations for Estimating Carbon Stocks*. [Online]. Available: https://winrock.org/wp-content/uploads/2018/08/Winrock-Guidance-on-calculating-carbon-stocks-1.pdf [Accessed June. 22, 2024].

[28] Intarat, K. and Vaiphasa, C., (2020). Modeling Mangrove Above-Ground Biomass Using Terrestrial Laser Scanning Techniques: A Case Study of the Avicennia marina Species in the Bang Pu District, Thailand. *International Journal of Geoinfo*rmatics, Vol. 16(2), 53–62. https://journals.sfu.ca/ijg/index.php/journal/article/view/1817.

[29] Shao, Z. and Zhang, L., (2016). Estimating Forest Aboveground Biomass by Combining Optical and SAR Data: A Case Study in Genhe, Inner Mongolia, China. *Sensors (Switzerland)*, Vol. 16(6). https://doi.org/10.3390/s16060834.

[30] Cutler, M. E. J., Boyd, D. S., Foody, G. M. and Vetrivel, A., (2012). Estimating Tropical Forest Biomass with a Combination of SAR Image Texture and Landsat TM Data: An Assessment of Predictions between Regions. *ISPRS Journal of Photogrammetry and Remote Sensing*, Vol. 70, 66–77. https://doi.org/10.1016/j.isprsjprs.2012.03.011.

[31] Alebele, Y., Zhang, X., Wang, W., Yang, G., Yao, X., Zheng, H., Zhu, Y., Cao, W. and Cheng, T., (2020). Estimation of Canopy Biomass Components in Paddy Rice from Combined Optical and SAR Data Using Multi-Target Gaussian Regressor Stacking. *Remote Sensing (Basel)*, Vol. 12(16). https://doi.org/10.3390/rs12162564.

[32] Mansaray, L. R., Zhang, K. and Kanu, A. S., (2020). Dry Biomass Estimation of Paddy Rice with Sentinel-1A Satellite Data Using Machine Learning Regression Algorithms. *Computers and Electronics in Agriculture*, Vol. 176. https://doi.org/10.1016/j.compag.2020.105674.

[33] Panday, U. S., Shrestha, N., Maharjan, S., Pratihast, A. K., Shahnawaz, Shrestha, K. L. and Aryal, J., (2020). Correlating the Plant Height of Wheat with Aboveground Biomass and Crop Yield Using Drone Imagery and Crop Surface Model, A Case Study from Nepal. *Drones*, Vol. 4(3), 1–15. https://doi.org/10.3390/drones4030028.

[34] Joshi, A. M., Shahnawaz, S. and Ranjit, B., (2019). Estimating above Ground Biomass of Pinus Roxbhurghii Using Slope Based Vegetation Index Model. *ISPRS Annals of the Photogrammetry, Remote Sensing and Spatial Information Sciences, Copernicus GmbH*, Vol. IV-5/W2, 35–42. https://doi.org/10.5194/isprs-annals-IV-5-W2-35-2019.

[35] Yuzugullu, O., Erten, E. and Hajnsek, I., (2017). Estimation of Rice Crop Height from X-and C-Band PolSAR by Metamodel-Based Optimization. *IEEE Journal of Selected Topics in Applied Earth Observations and Remote Sensing*, Vol. 10(1), 194–204. https://doi.org/10.1109/JSTARS.2016.2575362.

[36] Thapa, R. B., Itoh, T., Shimada, M., Watanabe, M., Takeshi, M. and Shiraishi, T., (2014). Evaluation of ALOS PALSAR Sensitivity for Characterizing Natural Forest Cover in Wider Tropical Areas. *Remote Sensing of Environment*, Vol. 155, 32–41. https://doi.org/10.1016/j.rse.2013.04.025.

[37] Suwanprasit, C. and Strobl, J., (2020). Aboveground Biomass Estimation in an Upland Tropical Evergreen Forest Environment from Landsat 7 ETM+. *International Journal of Geoinformatics*, Vol. 16(4), 39–50. https://journals.sfu.ca/ijg/index.php/journal/article/view/1795.

[38] Dwivedi, M., Saxena, S., Neetu, and Ray, S. S., (2019). Assessment of Rice Biomass Production and Yield Using Semi-Physical Approach and Remotely Sensed Data. *International Society for Photogrammetry and Remote Sensing*, Vol. 217–222. https://doi.org/10.5194/isprs-archives-XLII-3-W6-217-2019.

[39] Ubon, B., Amkha, S. and Smakgahn, K., (2012). Effects of Tillage and Plant Residue Management on Growth, Yield and Carbon Stock in Plant and Soil Under Rice Production. *Thai Journal of Soils and Fertilizers (Thailand)*, Vol. 34, 17–26. https://kuojs.lib.ku.ac.th/index.php/tjsf/article/view/4383/2052.

[40] Keophila, M., Thammasome, N., Lawongsa, P., Tulaphitak, D. and Dejphimon, K., (2013). Rice Straw Rates Influencing Rice Yields and Greenhouse Gases. *Khon Kaen Agriculture Journal*, Vol. 41, 33–38. https://ag2.kku.ac.th/kaj/PDF.cfm?filename=04%2033-38.pdf&id=1076&keeptrack=9&fbclid=IwZXh0bgNhZW0CMTAAAR0znVJpqW_znS5fApBOzVdz_ADgWadIJDPVoDEWTdRKYPlnqZwwTfp-ZwI_aem_CchzImBjlW5hvMOTo6D_Lg.

[41] Wiseman, G., McNairn, H., Homayouni, S. and Shang, J., (2014). RADARSAT-2 Polarimetric SAR Response to Crop Biomass for Agricultural Production Monitoring. *IEEE Journal of Selected Topics in Applied Earth Observations and Remote Sensing*, Vol. 7(11), 4461–4471. https://doi.org/10.1109/JSTARS.2014.2322311.

[42] Parracciani, C., Gigante, D., Bonini, F., Grassi, A., Morbidini, L., Pauselli, M., Valenti, B., Lilli, E., Antonielli, F. and Vizzari, M., (2024). Leveraging Google Earth Engine for a More Effective Grassland Management: A Decision Support Application Perspective. *Sensors*, Vol. 24(3). https://doi.org/10.3390/s24030834.

[43] Poortinga, A., Clinton, N., Saah, D., Cutter, P., Chishtie, F., Markert, K. N., Anderson, E. R., Troy, A., Fenn, M., Tran. L. H., Bean, B., Nguyen, Q., Bhandari, B., Johnson, G. W. and Towashiraporn, P., (2018). An Operational Before-After-Control-Impact (BACI) Designed Platform for Vegetation Monitoring at Planetary Scale. *Remote Sensing (Basel)*, Vol. 10(5). https://doi.org/10.3390/rs10050760.

[44] Markert, K. N., Schmidt, C. M., Griffin, R. E., Flores, A. I., Poortinga, A., Saah, D. S., Muench, R. E., Clinton, N. E., Chishtie, F., Kityuttachai, K., Someth, P., Anderson, E., Aekakkararungroj, A. and Ganz, D., (2018). Historical and Operational Monitoring of Surface Sediments in the Lower Mekong Basin Using Landsat and Google Earth Engine Cloud Computing. *Remote Sensing (Basel)*, Vol. 10(6). https://doi.org/10.3390/rs10060909.